On the generation of turbulent inflow conditions for boundary layer simulations

By T. S. Lund, X. Wu[1], AND K. D. Squires[1]

1. Motivation and objectives

Turbulent flows that exhibit inhomogeneities in the streamwise direction pose a particular challenge to numerical simulation approaches due to the need to prescribe time-dependent turbulent inflow conditions. In most cases the flow downstream is more or less "driven" by the conditions at the inlet, making it necessary to specify realistic turbulent fluctuations that are in equilibrium with the assumed mean flow. This requirement often dictates that the inflow data should satisfy the Navier-Stokes equations, which in turn implies that an independent simulation be used to generate them. Detailed simulations for the purpose of creating inflow conditions can be costly and thus certain levels of approximation are desirable. In this paper we shall focus on an approximate yet accurate method for generating inflow conditions for spatially-developing boundary layer simulations. The proposed method is essentially a simplification of the method of Spalart and Leonard (1985), who devised an ingenious transformation that allows for the calculation of spatially-evolving boundary layers in conjunction with periodic boundary conditions applied in the streamwise direction. While this method is elegant and highly accurate, it is more complicated than is necessary for the purpose of generating inflow data. A few key approximations are used in this work to arrive at a "modified Spalart method" that is very easy to implement and efficient to use. The new method is shown to yield results that compare well with the computations of Spalart (1988). When used as a means of generating inflow data, the modified Spalart method is shown to be superior to existing approaches.

2. Accomplishments

2.1 Review of Spalart's original method

The basic idea behind the method of Spalart and Leonard (1985) is to define a set of coordinate lines along which the streamwise inhomogeneity associated with the boundary layer growth is minimized. When the Navier-Stokes equations are transformed into this coordinate system, the velocity field is approximately homogeneous in the streamwise direction and is thus amenable to periodic boundary conditions. The periodic boundary condition allow for a "self-contained" simulation that does not require external inputs for the upstream and downstream boundaries. In addition, periodic boundary conditions allow for the use of a highly-accurate Fourier

1 University of Vermont, Mechanical Engineering Department, Burlington, VT 05405

representation of the velocity field in the streamwise direction. While the advantages of periodic boundary conditions are apparent, they come at the expense of a more complicated set of equations to solve. The coordinate transformation introduces new terms to the Navier-Stokes equations that account for the inhomogeneity in the streamwise direction. These so-called "growth terms" are both numerous and complicated in form. Spalart was able to show that a few of the terms are of higher order and therefore could be neglected. Several terms still remain, however, and these involve streamwise gradients of the mean flow variables, which must be supplied externally. In his 1988 work, Spalart advocates deducing these quantities from two or more simulations performed at different Reynolds numbers.

2.2 Proposed modification to Spalart's method

The main disadvantage of Spalart's method is the need evaluate the growth terms. The presence of these terms require a special flow solver along with possibility of having to perform multiple simulations in order to estimate streamwise gradients of the mean flow quantities. In this section we propose a modification of Spalart's method that effectively eliminates the need to deal with the growth terms. This is achieved by electing to transform only the boundary conditions as opposed to the entire solution domain. In effect, the proposed method computes a spatially-evolving boundary layer in a Cartesian coordinate system but makes use of the ideas of Spalart and Leonard to create a quasi-periodic boundary condition in the streamwise direction. This approach has the advantage that an existing Cartesian inflow-outflow simulation code can be adapted for the purpose of inflow generation by straightforward modifications to the streamwise boundary conditions. Furthermore, the spatial development of the boundary layer is computed directly and only a single empirical relation is required to relate the wall shear at the inlet boundary to the solution downstream.

Our simplifications come at the expense of the loss of strict periodic boundary conditions in the streamwise direction and therefore the inability to use a Fourier representation. This is not a concern in the context of inflow generation, however, since the recipient spatially-evolving simulation will invariably use discrete operators. There is little to be gained from generating inflow data with a numerical method that is significantly more accurate than what is to be used in the main simulation. In fact, our experience has been that non-physical transients often arise near the inlet boundary when inflow data generated with a high fidelity method are subjected to the increased numerical errors associated with the use of lower-order approximations in the inflow-outflow simulation.

The heart of our method is a means of estimating the velocity at the inlet plane based on the solution downstream. This is accomplished through the use of classical scaling laws for an equilibrium turbulent boundary layer. The procedure is to extract the velocity from a plane near the domain exit, rescale it, and then reintroduce it as a boundary condition at the inlet. Following Spalart & Leonard (1985), we first decompose the velocity into a mean and fluctuating part and then apply the appropriate scaling laws to each component separately.

The decomposition is achieved by defining the mean (denoted by upper case) as

an average in the spanwise direction and in time. The velocity fluctuation is then defined as

$$u_i'(x,y,z,t) = u_i(x,y,z,t) - U_i(x,y) \ . \tag{1}$$

In an effort to simplify the notation, the overline denoting the LES filter is omitted on u_i throughout this section.

The mean flow is rescaled according to the law of the wall in the inner region and the defect law in the outer region. The law of the wall reads

$$U^{\text{inner}} = u_\tau(x) f_1(y^+) \ , \tag{2}$$

where $u_\tau = \sqrt{\nu(\partial u/\partial y)_{\text{wall}}}$ is the friction velocity, $y^+ = (u_\tau y)/\nu$ is the wall coordinate, and f_1 is a universal function to be determined. The defect law is

$$U_\infty - U^{\text{outer}} = u_\tau(x) f_2(\eta) \ , \tag{3}$$

where $\eta = y/\delta$ is the outer coordinate (δ is the boundary layer thickness), U_∞ is the free-stream velocity, and f_2 is a second universal function to be determined. Let U_{recy} and U_{inlt} denote the mean velocity at the downstream station to be recycled, and at the inlet respectively. The law of the wall, (2), and the defect law, (3), dictate that U_{recy} and U_{inlt} are related in the inner and outer regions via

$$U_{\text{inlt}}^{\text{inner}} = \gamma U_{\text{recy}}(y_{\text{inlt}}^+) \tag{4}$$

and

$$U_{\text{inlt}}^{\text{outer}} = \gamma U_{\text{recy}}(\eta_{\text{inlt}}) + (1-\gamma) U_\infty \ , \tag{5}$$

where

$$\gamma = \left(\frac{u_{\tau,\text{inlt}}}{u_{\tau,\text{recy}}} \right) \ . \tag{6}$$

The independent variables in (4) and (5), y_{inlt}^+ and η_{inlt}, are the inner and outer coordinates of the grid nodes at the inlet station. Thus, $U_{\text{recy}}(y_{\text{inlt}}^+)$ is the mean velocity at the recycle station, expressed as a function of y^+, and evaluated at the inner coordinate of the mesh at the inlet. This evaluation requires an interpolation since the inner coordinates for the grid nodes at the recycle and inlet stations will, in general, be different. A linear interpolation was found to be sufficiently accurate for this purpose. A similar interpolation is required for the outer coordinate.

The mean vertical velocity in the inner and outer regions is assumed to scale as

$$V^{\text{inner}} = U_\infty f_3(y^+) \ , \tag{7}$$

and

$$V^{\text{outer}} = U_\infty f_4(\eta) \ , \tag{8}$$

where f_3 and f_4 are assumed to be universal functions. Applied between the recycle and inlet stations, the above scaling laws lead to

$$V_{\text{inlt}}^{\text{inner}} = V_{\text{recy}}(y_{\text{inlt}}^+) \ , \tag{9}$$

and

$$V_{\rm inlt}^{\rm outer} = V_{\rm recy}\left(\eta_{\rm inlt}\right) \ . \tag{10}$$

The spanwise velocity should be zero in the mean and thus no scaling relations are required.

The velocity fluctuations in the inner and outer regions are decomposed further to give

$$(u_i')^{\rm inner} = u_\tau(x) g_i(x, y^+, z, t) \ , \tag{11}$$

and

$$(u_i')^{\rm outer} = u_\tau(x) h_i(x, \eta, z, t) \ . \tag{12}$$

The purpose of this decomposition is to isolate the streamwise inhomogeneity through the explicit dependence on u_τ. The functions g_i and h_i are then approximately homogeneous in the streamwise direction and are therefore amenable to periodic boundary conditions. In Spalart & Leonard (1985) and Spalart (1988), periodic boundary conditions are assumed at this stage. The procedure here is different since we have elected to retain an inflow-outflow structure. The fundamental difference in the present approach is that the "periodic" condition provides only one-way coupling between the recycle station and the inlet. The velocity fluctuations at the downstream station will be related to those at the inlet using (11) and (12), but there is no downstream transfer of information from the inlet via boundary conditions. A convective outflow condition applied at the domain exit provides the necessary downstream boundary condition.

Assuming the functions g_i and h_i to be "periodic" the velocity fluctuations at the inlet are related to those at the recycle station via

$$(u_i')_{\rm inlt}^{\rm inner} = \gamma\,(u_i')_{\rm recy}\left(y_{\rm inlt}^+, z, t\right) \ , \tag{13}$$

and

$$(u_i')_{\rm inlt}^{\rm outer} = \gamma\,(u_i')_{\rm recy}\left(\eta_{\rm inlt}, z, t\right) \ . \tag{14}$$

Equations (4), (5), (6), (9), (10), (13), and (14) provide a means of rescaling the mean and fluctuating velocity for both the inner and outer regions of the boundary layer. A composite profile that is approximately valid over the entire layer is obtained by forming a weighted average of the inner and outer profiles:

$$(u_i)_{\rm inlt} = \left[(U_i)_{\rm inlt}^{\rm inner} + (u_i')_{\rm inlt}^{\rm inner}\right]\left[1 - W\left(\eta_{\rm inlt}\right)\right] \ + \ \left[(U_i)_{\rm inlt}^{\rm outer} + (u_i')_{\rm inlt}^{\rm outer}\right] W\left(\eta_{\rm inlt}\right) . \tag{15}$$

The weighting function $W(\eta)$ is defined as

$$W(\eta) = \frac{1}{2}\left\{1 + \frac{\tanh\left[\frac{\alpha(\eta - b)}{(1-2b)\eta + b}\right]}{\tanh(\alpha)}\right\} \ , \tag{16}$$

where $\alpha = 4$ and $b = 0.2$. The weighting function is zero at $\eta = 0$, 0.5 at $\eta = b$, and unity at $\eta = 1$. The parameter α controls the width of the region over which

the function transitions from 0 to 1. For $\alpha \to \infty$ the distribution becomes a step function centered at $\eta = b$. As $\alpha \to 0$ the transition is spread across the entire boundary layer. The values of α and b quoted above were determined through analysis of an independent spatially-evolving boundary layer simulation.

The rescaling operation requires the scaling parameters u_τ and δ both at the recycle station and at the inlet. These quantities can be determined from the mean velocity profile at the rescale station, but must be specified at the inlet. It turns out that the problem is over determined if both u_τ and δ are fixed independently at the inlet, and thus an additional relation is needed to connect one of these parameters at the inlet to the solution on the interior. While several suitable relations exist, we have obtained the best results by fixing δ at the inlet and computing u_τ via

$$u_{\tau,\mathrm{inlt}} = u_{\tau,\mathrm{resc}} \left(\frac{\theta_{\mathrm{resc}}}{\theta_{\mathrm{inlt}}} \right)^{1/[2(n-1)]} ; \qquad n = 5, \tag{17}$$

where θ is the momentum thickness. The above relation is similar to the Ludwig-Tillmann (1949) correlation and can be derived from the standard power-law approximations $C_f \sim R_x^{-1/n}$, $\theta/x \sim R_x^{-1/n}$. In many cases it is more advantageous to control the inlet momentum thickness than the inlet boundary layer thickness. This can be done with a little extra effort by iteratively adjusting the inlet boundary layer thickness until the target inlet momentum thickness is achieved.

2.3 Numerical method

A second order finite difference method on a staggered mesh is used to discretize the incompressible Navier-Stokes equations (see Harlow & Welch, 1965). The fractional step method (e.g., see Chorin 1967, Kim & Moin 1985) is used to enforce the incompressibility constraint through the solution of a Poisson equation for the pressure. The discrete system is time advanced in a semi-implicit fashion where all terms with gradients in the wall-normal direction are treated implicitly with the Crank-Nicholson method while the remaining terms are treated explicitly with a third-order Runge-Kutta scheme.

The boundary conditions on the top surface of the computational domain are

$$\frac{\partial \overline{u}}{\partial y} = 0\,, \qquad \overline{v} = U_\infty \frac{d\delta^*}{dx}\,, \qquad \frac{\partial \overline{w}}{\partial y} = 0\,, \tag{18}$$

where δ^* is the boundary layer displacement thickness. The derivative $d\delta^*/dx$ is evaluated from the mean velocity field. At the exit plane a convective boundary condition of the form $\partial \overline{u}_i/\partial t + c\partial \overline{u}_i/\partial x = 0$ is applied (c is the local bulk velocity, Han *et al.* 1983).

The dynamic Smagorinsky model is use to model the effect of the unresolved motions. The equations for the model coefficient are averaged in the spanwise direction, and test filtering is performed in planes parallel to the wall (see Ghosal *et al.*, 1995 for more details).

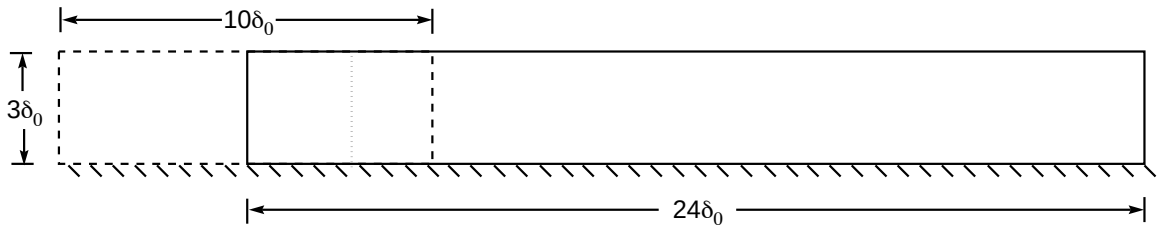

FIGURE 1. Arrangement of the computational domains. The solid lines represent the boundaries of the (inflow-outflow) boundary layer simulation while the dashed lines represent the inflow calculation using the modified Spalart method. The dotted line denotes the location of the recycle station in the inflow calculation.

2.4 Results

The methodology described above was used to simulate a zero pressure gradient turbulent boundary layer over a momentum thickness Reynolds number range of R_θ=1400-1640. As an example of use of this method for inflow generation, a time series of velocity data was extracted from the mid plane of the simulation and used as an inflow condition for an inflow-outflow simulation of a zero pressure gradient boundary layer. The latter simulation extends from R_θ=1530 to 2150. Due to the fact that the inflow data is extracted from the central plane of inflow generation simulation, the two domains overlap as depicted in Fig. 1. This feature provides a critical test for the inflow generation technique; the results should be nearly identical in the region of overlap, and no changes in the streamwise evolution of boundary layer statistics should occur as the flow develops further downstream.

In order to fully evaluate the inflow condition obtained using the modified Spalart method, calculations were also performed using inflow obtained from two simpler methods. The first of these is achieved by extracting velocity information from a parallel-flow boundary layer simulation. This simulation is similar to the modified Spalart method, except that strict periodic boundary conditions are applied in the streamwise direction. In addition, a no-stress condition is applied at the upper boundary along with the condition that the (instantaneous) vertical velocity vanish there. These boundary conditions are very easy to implement but result in a boundary layer that is void of spatial growth. This method has been used by Lund and Moin (1996) to generate inflow data for a boundary layer over a curved surface.

The second alternative set of inflow data was fabricated through the use of a random number generator. In this approach, both the mean and second order velocity statistics were constrained to match the profiles obtained from the modified Spalart method calculation. The random fluctuations are decorrelated in space and thus the synthetic velocity field lacks turbulent structure. A similar method has been used by Le and Moin (1994) and Akselvoll and Moin (1995) to produce inflow conditions for simulations of a backward-facing step.

The computational domains for the inflow generation and the recipient spatially-evolving simulation have dimensions $10\delta_0 \times 3\delta_0 \times (\pi/2)\delta_0$ and $24\delta_0 \times 3\delta_0 \times (\pi/2)\delta_0$ in the streamwise, wall-normal, and spanwise directions, respectively, where δ_0 is the

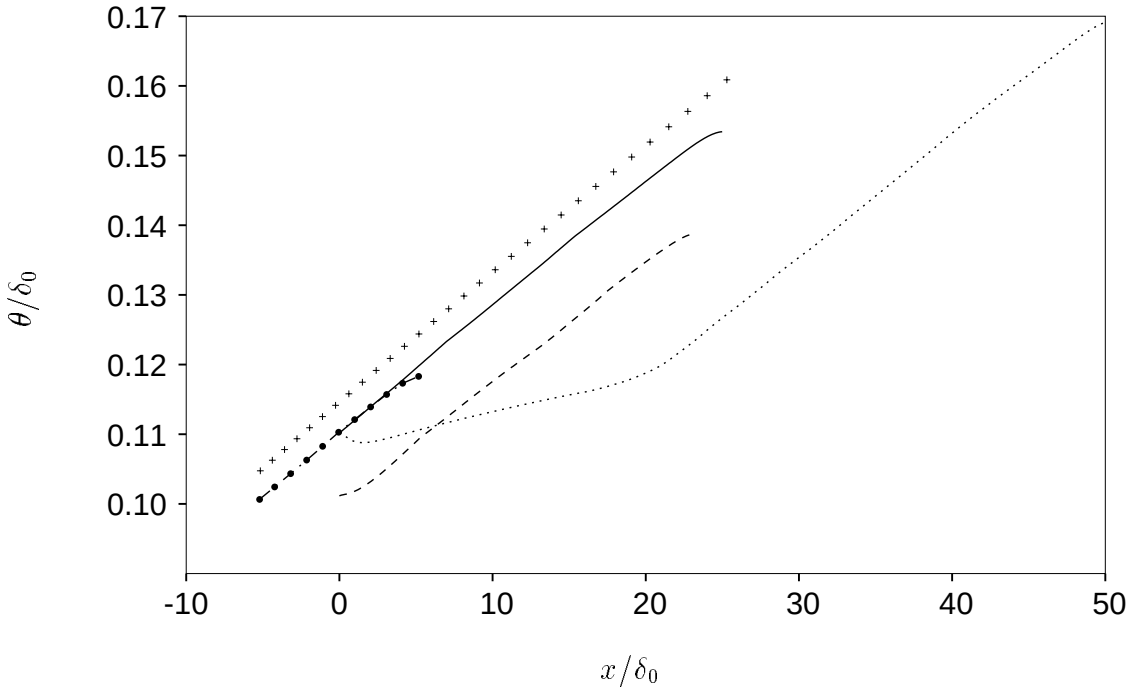

FIGURE 2. Evolution of the momentum thickness in the inflow-outflow simulations. ——— , inflow generated with the modified Spalart method; – – – – , inflow generated with the parallel-flow boundary layer method; ····· , inflow generated with the random fluctuation inflow method; —●– –●— , momentum thickness from the inflow calculation using the modified Spalart method; + , momentum integral estimate.

99% boundary layer thickness at the inlet of the main simulation. The two meshes contains $100 \times 45 \times 64$ and $240 \times 45 \times 64$points in the streamwise, wall-normal, and spanwise directions. The mesh spacings are the same for the two grids and have the following dimensions in wall units: $\Delta x^+ \approx 64$, $\Delta y^+_{\text{wall}} \approx 1.2$, and $\Delta z^+ \approx 15$. The mesh is uniform in the streamwise and spanwise directions while a hyperbolic tangent stretching is used in the normal direction to cluster points near the wall.

Once the modified Spalart and parallel-flow boundary layer simulations had reached a statistically stationary state, a time sequence of two-dimensional velocity fields was extracted from the central $x-z$ (streamwise-spanwise) plane and written to disk. The inflow-outflow calculations were then performed by reading one plane of inflow data per time step. The inflow-outflow simulations were run for an initial period of 70 inertial time units (U_∞/δ_0), or equivalently 2.9 flow through times (U_∞/X_L), to eliminate starting transients. Statistics were then accumulated over a period of 1400 inertial time units.

Figure 2 shows the evolution of the momentum thickness for the three inflow-outflow simulations as well as the modified Spalart method calculation. For reference, the predictions of a momentum integral estimate (White, 1974) are also included. The first thing to notice is that the results from the modified Spalart method calculation and its corresponding inflow-outflow simulation agree quite well

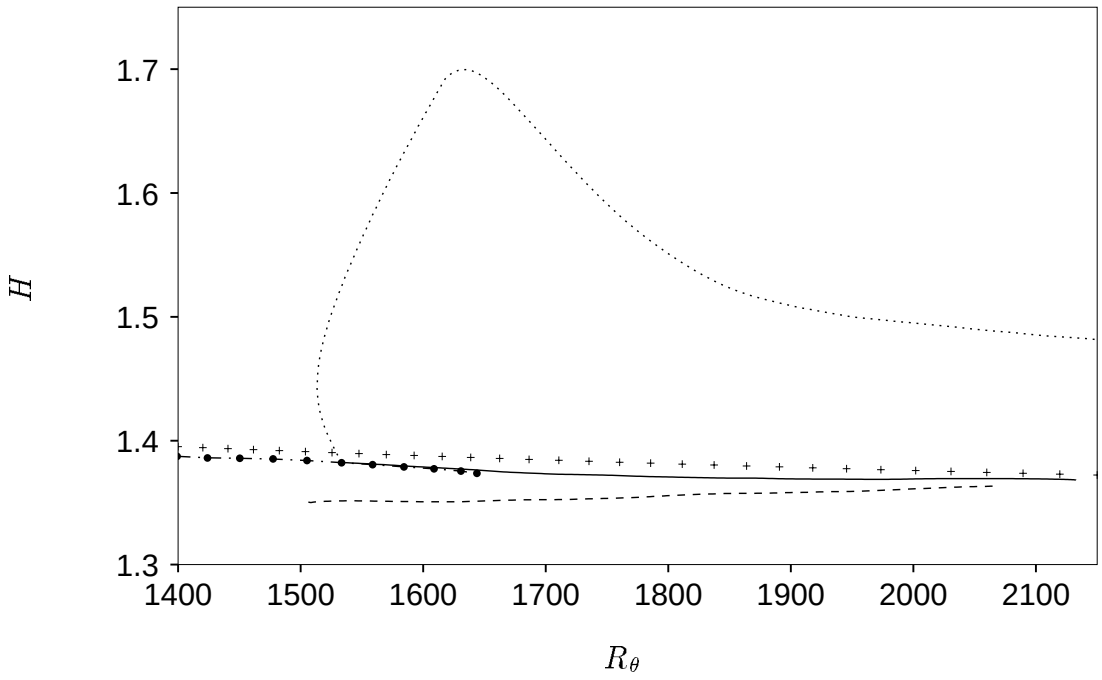

FIGURE 3. Evolution of the shape factor in the inflow-outflow simulations. ——— , inflow generated with the modified Spalart method; – – – – , inflow generated with the parallel-flow boundary layer method; ····· , inflow generated with the random fluctuation inflow method; –●– – ●– , shape factor from the inflow calculation using the modified Spalart method; + , momentum integral estimate.

in region of overlap ($x/\delta_0 = 0 - 5$). The small deviation near the downstream end of the inflow calculation ($x/\delta_0 \simeq 5$) is due to errors produced by the exit boundary condition. A similar decrease in slope is noted near the end of the main simulation. Aside from this small deviation, the momentum thickness evolution shows no sign of readjustment with downstream distance and agrees well with the momentum integral estimate. The parallel-flow method yields a momentum thickness distribution that is reasonable although there is a noticeable transient near the inlet. The agreement with the momentum integral analysis is also not as good as compared with the case using the modified Spalart inflow data.

While the modified Spalart method and the parallel-flow method produce reasonable results, the random fluctuation method is seen to lead to a very pronounced transient where the initial growth rate is almost a factor of four too small. This feature is due to the fact that the pseudo-turbulence produced by the random fluctuations is not a solution to the Navier-Stokes equations. The fluctuations decay under the influence of viscosity until physical instabilities organize the disturbances into realistic turbulence. This process results in a transition of sorts that is responsible for the change in slope of the momentum thickness at $x/\delta_0 \simeq 20$. Once this transition is past, the growth rate is greatly improved and is comparable to the results of the other simulations. Note that the computational domain for the

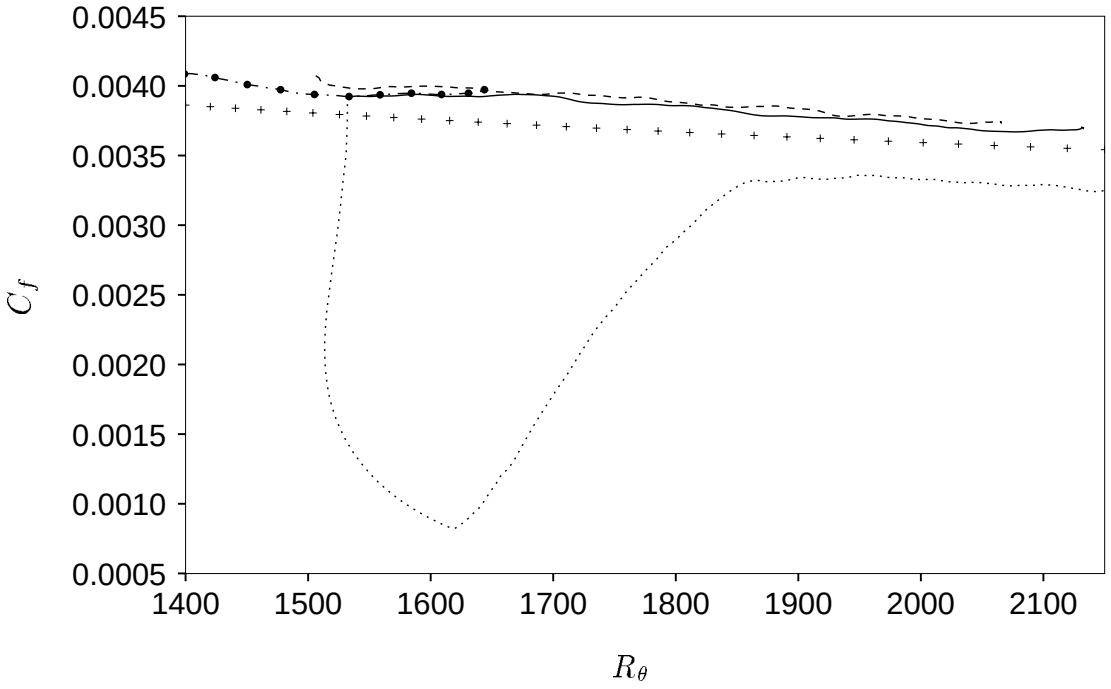

FIGURE 4. Evolution of the skin friction in the inflow-outflow simulations. ——— , inflow generated with the modified Spalart method; - - - - , inflow generated with the parallel-flow boundary layer method; ····· , inflow generated with the random fluctuation inflow method; -●--● , skin friction from the inflow calculation using the modified Spalart method; + , momentum integral estimate.

random fluctuation inflow case extends more than twice as far downstream as the other two cases ($x/\delta_0 = 50$ as opposed to $x/\delta_0 = 50$). This was done in order to compensate for the initial slow growth in the momentum thickness so that all three simulations cover roughly the same momentum thickness Reynolds number range.

The shape factor (ratio of displacement to momentum thickness) evolution is shown in Fig. 3. As in the case of the momentum thickness, the modified Spalart calculation and its corresponding inflow-outflow simulation are in good agreement within the overlap region. The results are also in very good agreement with the momentum integral estimate. When the parallel-flow method is used, the shape factor is a few percent low at the inlet but this error diminishes with increasing streamwise distance. The results from the random fluctuation method are again poor. The shape factor increases initially toward the laminar value of 2.6, then following "transition" relaxes back toward more reasonable values for a turbulent boundary layer. Note however that the 50 boundary layer thicknesses of spatial evolution are not sufficient to produce a canonical turbulent boundary layer when this method is used.

Figure 4 shows the computed skin friction. Once again the results from the modified Spalart simulation and its inflow-outflow counterpart are seen to be in good agreement within the region of overlap. They are also in reasonable agreement

with the momentum integral estimate. The parallel-flow method produces a small initial transient, followed by an acceptable skin friction evolution. The random fluctuation method exhibits an initial sharp drop in skin friction followed by an increase once the flow develops realistic turbulent structure.

Mean velocity profiles for three streamwise locations are shown in Fig. 5. The simulation with inflow obtained using the modified Spalart method (Fig. 5a) yields canonical mean profiles as the flow evolves downstream. In particular, the viscous sublayer and logarithmic region collapse very well when plotted in wall units, while the expected Reynolds number dependence is displayed in the wake region. The results also agree well with the computations of Spalart (1988), except at the beginning of the logarithmic region where the mean velocity is overpredicted slightly. This defect is a common feature of simulations using finite-difference methods on relatively coarse meshes and is not related to the rescaling approach used in the inflow generation process. In support of this claim, we include the results of Rai & Moin (1993) which display a very similar discrepancy in the same region of the profile.

The simulation with the parallel-flow method (Fig. 5b) is seen to produce a small transient where the initial profile shape changes in the logarithmic and wake regions. The parallel-flow method produces a profile that has a larger deviation in the logarithmic region. This discrepancy diminishes with increasing streamwise distance and the profiles at the last two stations collapse in the logarithmic region. These latter two profiles are also nearly identical to the corresponding pair in the case with the modified Spalart method inflow (Fig. 5a).

The random fluctuation method (Fig. 5c) leads to rather anomalous behavior where the profile experiences a large transient as it evolves downstream. At the second plotting station, the mean velocity is underpredicted in the logarithmic region and an unusually large wake develops. The profile then starts to relax back to the expected shape with an increase of the velocity in the logarithmic region and a reduction in the wake. The apparent agreement with the standard logarithmic law (between $y^+ = 30$ and 60) for the third plotting station is fortuitous; profiles further downstream show an overprediction in this region similar to that in the other two simulations. Consistent with this observation is the fact that the profiles do not reach a self-similar state by the domain exit, although it is roughly 50 initial boundary layer thicknesses downstream of the inlet.

Figure 6 shows velocity fluctuation and shear stress profiles for three streamwise locations. When inflow from the modified Spalart method is used (Fig. 6a), the profiles collapse reasonably well for the three Reynolds numbers and the results are in good agreement with the computations of Spalart (1988).

Simulations performed using the parallel-flow inflow (Fig. 6b) also results in profiles that yield an acceptable degree of collapse. The largest discrepancy occurs in the outer region of the streamwise and spanwise profiles where the values from the first station are too large. This is a side effect of the boundary conditions used in the inflow generation simulation. When the parallel-flow method is used, the

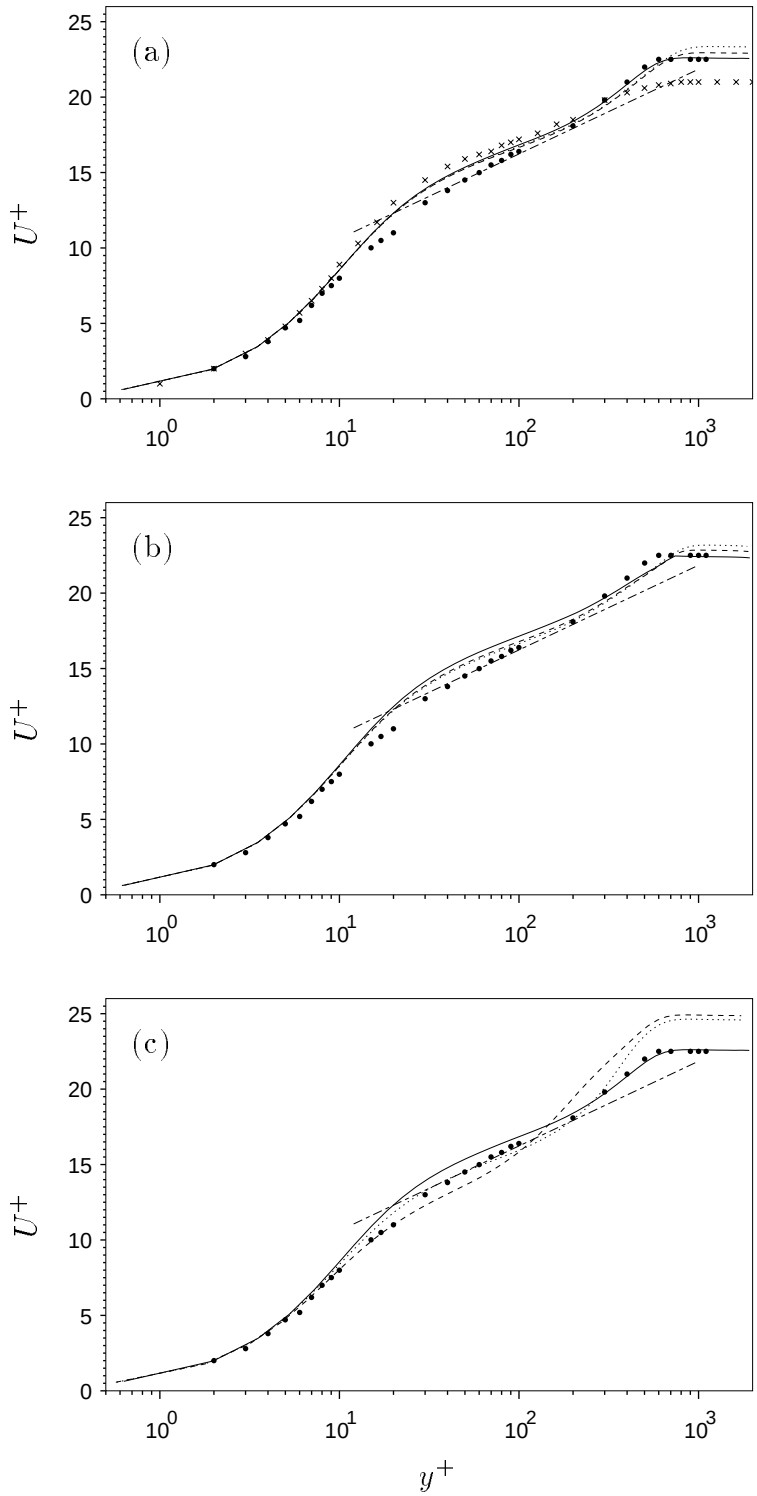

FIGURE 5. Mean velocity profiles in the inflow-outflow simulations. (a), inflow generated with the modified Spalart method; (b), inflow generated with the parallel-flow boundary layer method; (c), inflow generated with the random fluctuation method. ——— , $R_\theta = 1530$; - - - - , $R_\theta = 1850$; ····· , $R_\theta = 2050$; • , Spalart (1988), $R_\theta = 1410$; ×, Rai & Moin (1993), $R_\theta = 1350$.

boundary layer edge is rigidly defined as the position where the no stress, zero normal velocity boundary conditions are applied. This condition forces v' to vanish at the boundary layer edge and results in a redistribution of the wall-normal fluctuation energy into u' and w'. Another side effect of this approach is that there are no naturally occurring fluctuations in the region between the boundary layer edge and the upper boundary of the computational domain at the inflow plane. In an attempt to remedy this, random fluctuations were superimposed on the free-stream velocity in this region. The scaling of these disturbances is rather arbitrary, and in this case, the isotropic distribution $u_i' = 0.1U_\infty \exp[-2(y/\delta - 1)]$ was used. The high-frequency random disturbances decay rapidly, and after a few boundary layer thicknesses of spatial evolution, roughly the correct level of free-stream fluctuations are obtained. Aside from the problems near the boundary layer edge, the remainder of the profiles collapse reasonably well and are in acceptable agreement with Spalart (1988).

As in the case of the mean velocity profile, the results from the simulation using the random fluctuation method (Fig. 6c) are poor. The velocity fluctuations in the outer region of the profile are seen to decay initially and then rebuild as the streamwise distance is increased. The transient process is seen to be slow with the fluctuations not returning to equilibrium by the third plotting station which is roughly 35 initial boundary layer thicknesses downstream of the inlet.

3. Conclusions and future work

The proposed simplification to Spalart's method is seen to produce an accurate description a turbulent boundary layer. When used as a means of generating turbulent inflow data for inflow-outflow simulations of spatially-developing boundary layers, the method proves to be very effective at producing simulation results that are free of transients near the inlet boundary. A comparison of this method with the simpler parallel-flow or random fluctuation methods shows that it is superior to both of these techniques. The differences between the modified Spalart method and the parallel flow method are not so great, however, and the latter method may be acceptable in certain cases. The random fluctuation method, on the other hand, appears to be a very rough procedure when compared to the other two methods. Although the inflow data can be generated with minimal computational effort when this scheme is used, the resulting velocity field lacks turbulent structure. This fact implies that the inflow data must be allowed to evolve for a substantial streamwise distance before it can be subjected to an inhomogeneity. When the random fluctuation method has been used in the past, the inlet of the computational domain was displaced 10 to 20 boundary layer thickness upstream of the region of interest (Le and Moin, 1994; Akselvoll and Moin, 1995). The need to extend the mesh for the inflow-outflow simulation increases the overall cost, which obscures any savings in the generation of the inflow data. In fact, the incremental cost of enlarging the main simulation domain will probably exceed the cost to generate more accurate inflow in most cases.

In the future, the modified Spalart method will be generalized to allow for inclusion of a streamwise pressure gradient. This feature is useful for inflow-outflow

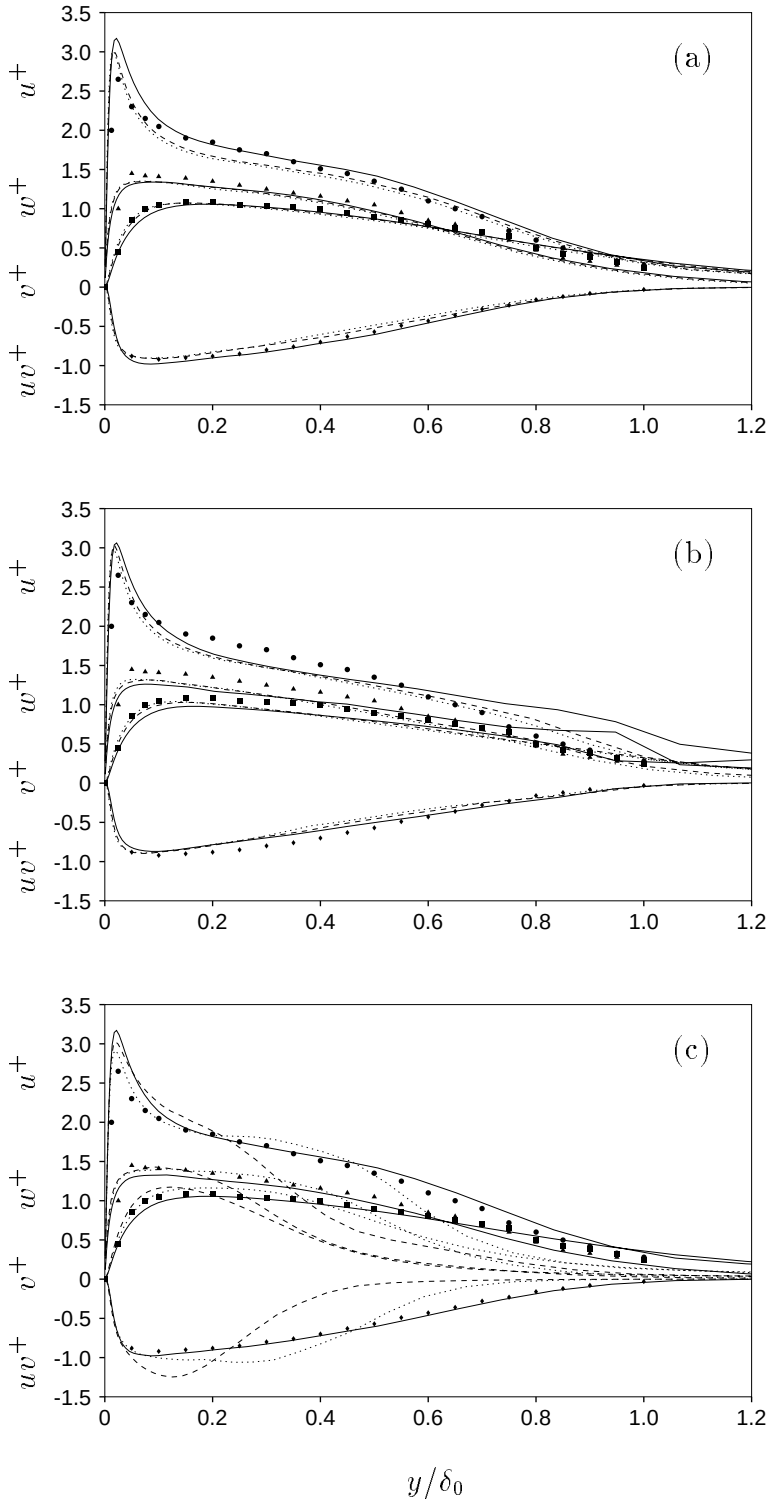

FIGURE 6. Velocity fluctuation and shear stress profiles in the inflow-outflow simulations. (a), inflow generated with the modified Spalart method; (b), inflow generated with the parallel-flow boundary layer method; (c), inflow generated with the random fluctuation method. ——— , $R_\theta = 1530$; - - - - , $R_\theta = 1850$; ····· , $R_\theta = 2050$. Filled symbols are data from the simulations of Spalart at $R_\theta = 1410$.

simulations where the inflow boundary is located in a region of significant pressure gradient. One relevant example is in the computation of the aft section of an airfoil. Previous attempts to simulate this flow (Kaltenbach and Choi, 1995; Jansen 1995) have shown that the computations are both costly and very sensitive to the details of the laminar-turbulent transition that takes place near the leading edge. Both of these problems can be minimized by electing to simulate only the aft section of the airfoil, since it is flow separation in this region that is of primary interest. Such a strategy has been adopted by Wang (this volume). In Wang's case the airfoil is at zero angle of attack and thus the pressure gradients are mild at the position where the inflow data are prescribed. At high angles of attack, however, the pressure gradients will be large at the inflow plane and it is desirable to have this effect captured in the inflow computation.

Preliminary study indicates that the modified Spalart method can be extended to account for a restricted class of equilibrium boundary layers that develop under power-law pressure gradients. Under these circumstances the same scaling laws described in this work continue to apply, and the required changes involve only a modification of the friction velocity computation at the inlet and the vertical velocity distribution at the upper boundary. These modifications will be made and the generalized method will be validated in one or more test cases before being used to generate inflow data for the truncated airfoil simulation.

REFERENCES

Akselvoll, K. & Moin, P. 1995 Large eddy simulation of turbulent confined coannular jets and turbulent flow over a backward facing step. Rep. TF-63, Thermosciences Div., Dept. Mech. Eng., Stanford University, Stanford, CA.

Chorin, A.J. 1967 A numerical method for solving incompressible viscous flow problems. *J. Comp. Phys.* **2,** 745-762.

Ghosal, S., Lund, T.S., Moin, P. & Akselvoll, K. 1995 A dynamic localization model for large-eddy simulation of turbulent flows. *J. Fluid Mech.* **286,** 229-255.

Han, T.Y., Meng, J.C.S. & Innis, G.E. 1983 An open boundary condition for incompressible stratified flows. *J. Comp. Phys.* **49,** 276-297.

Harlow, F.H. & Welch, J.E. 1965 Numerical calculation of time-dependent viscous incompressible flow of fluid with free surface. *Phys. Fluids.* **8,** 2182-2189.

Jansen, K. 1995 Preliminary large eddy simulation of flow around a NACA 4412 airfoil using an unstructured mesh. In *Annual Research Briefs 1995*, Center for Turbulence Research, Stanford Univ./NASA Ames, 61-72.

Kaltenbach, H.-J. & Choi, H. 1995 Large eddy simulation of flow around an airfoil on a structured mesh. In *Annual Research Briefs 1995*, Center for Turbulence Research, Stanford Univ./NASA Ames, 51-60.

KIM, J. & MOIN, P. 1985 Application of a fractional-step method to incompressible Navier-Stokes equations. *J. Comp. Phys.* **59,** 308-323.

LE, H. & MOIN, P. 1994 Direct numerical simulation of turbulent flow over a backward-facing step, Rep. TF-58, Thermosciences Div., Dept. Mech. Eng., Stanford University, Stanford, CA 94305.

LUDWIG, H. & TILLMANN, W. 1949 Untersuchungen uber die wandschubspannung turbulenter reibungsschichten. *Ing.-Arch.* **17,** 288-299. (trans. as NACA *Tech. Mem. 1285* (1949)).

LUND, T.S. & MOIN, P. 1996 Large eddy simulation of a concave wall boundary layer. *Int. J. of Heat and Fluid Flow.* **17,** 290-295.

RAI, M.M. & MOIN, P. 1993 Direct numerical simulation of transition and turbulence in a spatially evolving boundary layer. *J. Comp. Phys.* **109,** 169-192.

SPALART, P.R. & LEONARD, A 1985 Direct numerical simulation of equilibrium turbulent boundary layers, in *Proc. 5th Symp. on Turbulent Shear Flows*, Ithaca, NY, August 7-9, 1985. Bound volume published by Springer-Verlag, Berlin, 1987.

SPALART, P.R. 1988 Direct simulation of a turbulent boundary layer up to $Re_\theta = 1410$. *J. Fluid Mech.* **187,** 61-98.

WHITE, F.M., 1974 *Viscous Fluid Flow*, McGraw-Hill, New York.